ARCHIVES OF BIOCHEMISTRY AND BIOPHYSICS
Vol. 325, No. 2, January 15, pp. 199–208, 1996
Article No. 0025

Structural Studies of a Major Hemorrhagin (Rhodostoxin) from the Venom of *Calloselasma rhodostoma* (Malayan Pit Viper)

Maxey C. M. Chung,*[,1] Gnanajothy Ponnudurai,† Michihiko Kataoka,‡ Sakayu Shimizu,‡ and Nget-Hong Tan†

**Department of Biochemistry and Bioprocessing Technology Centre, National University of Singapore, Singapore 0511, Republic of Singapore; †Department of Biochemistry, University of Malaya, Kuala Lumpur, Malaysia; and ‡Department of Agricultural Chemistry, Kyoto University, Kyoto, Japan*

Received July 25, 1995, and in revised form October 17, 1995

The complete amino acid sequence, disulfide linkages, glycosylation sites, and carbohydrate structure of rhodostoxin, the major hemorrhagin from *Calloselasma rhodostoma* (Malayan pit viper), have been determined. This sequence confirmed the deduced amino acid sequence of the putative hemorrhagic protein encoded by the prorhodostomin cDNA of *C. rhodostoma*. Rhodostoxin contained four disulfide bonds that link Cys19–Cys60, Cys117–Cys198, Cys157–Cys182, and Cys159–Cys165. It is the first four-disulfide proteinase reported among all known venom metalloproteinases, which are either of the two-disulfide or three-disulfide type. Peptide-mapping and dot-blotting experiments showed the presence of two glycopeptides. Subsequent sequencing of these peptides established that the N-glycosylation sites are located at residues 91 and 181 of the amino acid sequence of the matured protein. Mass spectrometric analyses of these glycopeptides showed that they contain an oligosaccharide structure consisting of 4 units of *N*-acetylglucosamine, 5 units of hexose, 1 unit of fucose, and 2 units of neuraminic acids. The complete carbohydrate structure was then established by 2-D mapping analysis of the pyridylamino-oligosaccharides after hydrazinolysis and pyridylamination of the glycan chains.

Key Words: **hemorrhagin; *Calloselasma rhodostoma;* amino acid sequence; disulfide bridges; carbohydrate structure.**

General hemorrhagic syndrome is one of the characteristic symptoms associated with crotalid venom poisoning. The hemorrhagic activity of snake venom has been ascribed to the presence of hemorrhagins, which are metalloproteinases (1) that presumably act by destruction of the collagenous basement membrane and other connective tissue collagen with consequent weakening of the stability of the blood vessel causing hemorrhagic effects (2, 3). To date, more than 50 hemorrhagins have been purified from various snake venoms and the amino acid sequences of more than 10 hemorrhagins or related proteinases have been determined (4–12). The precise structure–function relationship of the hemorrhagins, however, remains to be elucidated. In addition, relatively little is known about the role and structure of the carbohydrate moieties of these metalloproteinases. In this paper, we report the amino acid sequence as well as the glycan structure of rhodostoxin, the major hemorrhagin of the Malayan pit viper (*Calloselama rhodostoma*) venom.

MATERIALS AND METHODS

Materials

Lyophilized *C. rhodostoma* venom was obtained from Latoxan (Rosans, France). Endoproteinase Lys C and 4-(aminosulfonyl)-7-fluoro-2,1,3-benzoxadiazole (ABD-F)[2] were from Wako Pure Chemicals (Japan), while trypsin, α-chymotrypsin, and thermolysin were from Boehringer-Mannheim. Protein/peptide sequencing reagents were from Applied Biosystems Inc. (Foster City, CA). HPLC solvents, trifluoroacetic acid and acetonitrile, were from either Sigma or Pierce and Merck or J. T. Baker, respectively. Shimpack CLC-ODS and TSK-gel Amide-80 columns were from Shimadzu and Tosoh, respectively. Sialidase (*Arthrobacter ureafaciens*), α-L-fucosidase (bovine kidney), β-galactosidase (bovine testis), and α-mannosidase (jack bean) were

[1] To whom correspondence should be addressed at Department of Biochemistry, Faculty of Medicine, National University of Singapore, Singapore 0511, Republic of Singapore. Fax: 65-7754933. e-mail: bchcm@leonis.nus.sg.

[2] Abbreviations used: ABD-F, 4-(aminosulfonyl)-7-fluoro-2,1,3-benzoxadiazole; TFA, trifluoroacetic acid; PA, pyridylamino.

0003-9861/96 $12.00

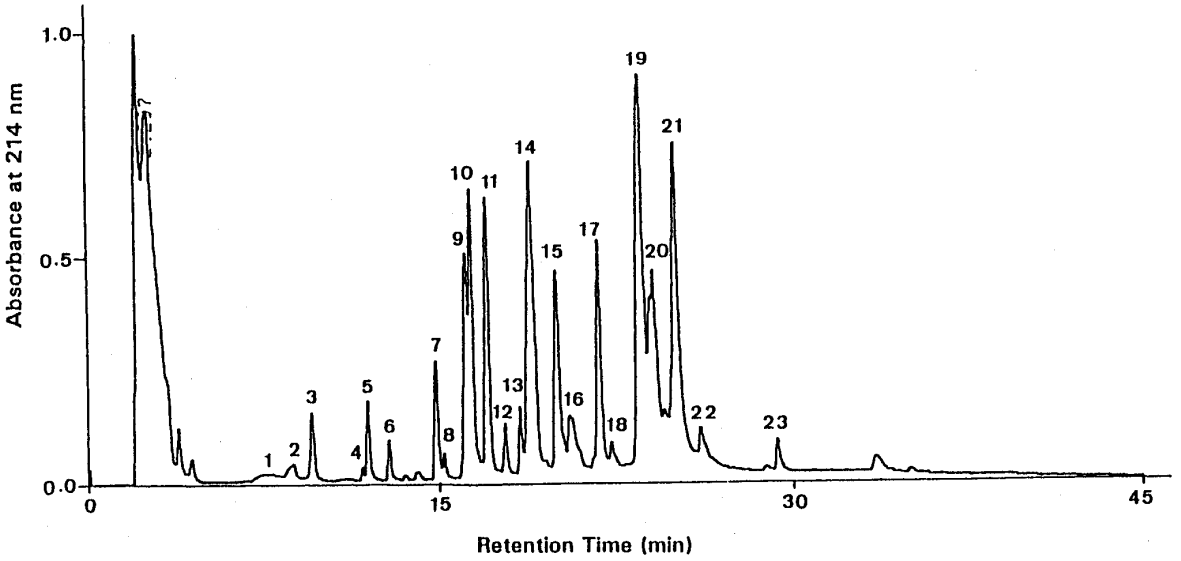

FIG. 1. HPLC elution profile of endoproteinase Lys-C digest of pyridylethylated rhodostoxin. For details of separation, see Materials and Methods.

purchased from Nacalai Tesque, Sigma, Boehringer-Mannheim, and Wako Pure Chemicals, respectively. α-2,3-Sialidase (*Salmonella typhimurium*) and lacto-*N*-biosidase (jack bean), β-galactosidase, and β-*N*-acetyl-hexosaminidase (jack bean) were obtained from Takara Shuzo and Seikagaku Co., respectively. All other chemicals (of analytical grades or of the highest grades available) were purchased from Sigma, BDH, or Aldrich.

Methods

(A) Protein Structure Analysis

(i) Peptide mapping. Rhodostoxin (~1 nmol) was reduced and pyridylethylated (13) and subsequently digested with endoproteinase Lys C at 37°C overnight in 10 mM Tris–HCl, pH 8.8, containing 4 M urea (substrate:enzyme ratio was 50:1). After digestion, peptides were fractionated by reversed-phase HPLC using a Vydac C_8 column (2.1 × 150 mm). The column was equilibrated with 0.1% TFA and eluted with a 45-min linear gradient of 0.1% TFA (buffer A) and 0.085% TFA in 70% acetonitrile (buffer B) at a flow rate of 0.2 ml/min. Peptides were monitored at 214 nm and were collected manually. Peptide purity was assessed by capillary electrophoresis (Model 270HT, Applied Biosystems Inc.) before sequencing. Heterogeneous peptides were further purified on a C_{18} Vydac column (2.1 × 150 mm) using the same buffer and flow rate as above.

(ii) Peptide sequencing. The N-terminal amino acid sequence and amino acid sequences of all the peptides were determined by using an Applied Biosystems 477A pulsed liquid-phase sequencer equipped with an on-line 120A PTH-amino acid analyzer.

(iii) Determination of disulfide bonds. The procedure adopted was based on that of Aitken *et al.* (14). Briefly, rhodostoxin (~1 nmol) was first alkylated with 4-vinylpyridine (without reduction) before being fragmented by cyanogen bromide [CNBr:protein, 10:1 (w/w) in 70% formic acid] for 48 h at room temperature in the dark. The CNBr-peptides were fractionated by HPLC on a 2.1 × 30-mm C_4 column (Applied Biosystems Inc.) using 0.1% TFA and 0.085% TFA/60% *n*-propanol as eluents at a flow rate of 0.3 ml/min. The absorbance was monitored at 230 nm. The purified CNBr-peptides were subsequently digested with trypsin in 100 mM ammonium bicarbonate, pH 7.8, containing 5 mM calcium chloride and 2 M urea at 37°C overnight. Tryptic peptides were purified using reversed-phase HPLC on a 2.1 × 100-mm column (C_8, RP-300, Applied Biosystems Inc.) using 0.1% TFA and 0.085% TFA/70% acetonitrile as chromatographic solvents. Cysteine-linked tryptic peptides were located by reacting half of the samples with a fluorescent label, ABD-F, based on the procedure of Kirley (15). After the reaction, labeled peptides (ABD-cys adduct) were identified by HPLC by either their absorption at 385 nm or emission at 520 nm. Subsequent amino acid sequencing of the remaining half of the relevant tryptic peptides allowed disulfide linkage assignments to be made.

(iv) Determination of carbohydrate content. The total hexose content of rhodostoxin was determined as described by Spiro (16).

(v) Deglycosylation. Rhodostoxin and its glycopeptides were deglycosylated using peptide-*N*-glycosidase F (PNGase) (Oxford Glycosystems) based on the manufacturer's recommendations. The molecular weight of deglycosylated hemorrhagin was determined by SDS–PAGE using the Laemmli procedure (17). The deglycosylated peptides were desalted by reversed-phase HPLC (C-18, 2.1 × 150 mm, Vydac) prior to amino acid sequencing.

(vi) Glycopeptide detection. This was performed essentially according to the procedure of Canas *et al.* (18). Briefly, HPLC-purified Lys C peptides were first partially dried and applied to a piece of prewetted Immobilon-AV membrane (Millipore). After a drying, blocking, and washing step, the membrane was stained with an amplified staining technique consisting of biotinylated lectins, avidin, and biotinylated peroxidase (19). Positively stained peptide(s) was used for sequencing to locate the glycosylation site(s) of the toxin.

(B) Structure of Glycan Chain

(i) Mass spectrometry. Glycopeptides (K-9 and K-14) dissolved in 0.1% (v/v) acetic acid were subjected to mass spectrometric analyses using a PE SCIEX API (atmospheric pressure ionization) III MS system. The sample was injected into the interface by a mobile phase consisting of 0.1% (v/v) acetic acid/20% (v/v) acetonitrile. Flow rate during the injection was 20 μl/min, and 5 μl was injected through a sample loop.

(ii) Isolation and pyridylamination of sugar chains of rhodostoxin. Oligosaccharides were released from rhodostoxin by hydrazinolysis

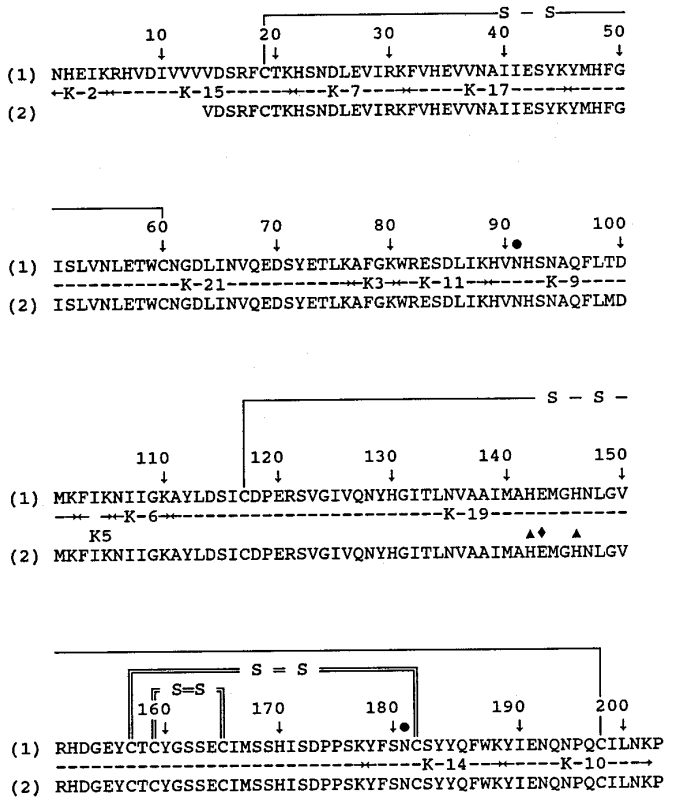

FIG. 2. Amino acid sequence, disulfide bridges and glycosylation sites of rhodostoxin. (1) indicates the amino acid sequence obtained by Edman sequencing of Lys C peptides. (2) indicates the amino acid sequence of the putative hemorrhagic protein deduced from the cDNA of prorhodostomin from *Calloselasma rhodostoma* venom. The two glycosylation sites at residues 91 and 181 are indicated by ●, while the two histidine residues proposed to be involved in zinc binding and the putative active site of the enzyme are represented by ▲ and ◆, respectively. Two disulfide linkages (Cys19–Cys60 and Cys117–Cys198) identified experimentally in this work are represented by single lines while the other two disulfide bridges (Cys157–Cys198 and Cys159–Cys165), identified based on homology with other hemorrhagins, are indicated by double lines.

and then were pyridylaminated according to Hase *et al.* (20). The pyridylamino derivatives of oligosaccharides were purified by gel filtration on a Sephadex G-15 column and were analyzed by a 2-D HPLC procedure as described in the next section.

(iii) 2-D mapping analysis of pyridylamino (PA)-oligosaccharides. Reverse-phase and size-fractionation HPLC were carried out on Shimpak CLC-ODS (0.6 × 15 cm) and TSK-gel Amide-80 (0.46 × 25 cm) columns, respectively, according to Tomiya *et al.* (21). PA-oligosaccharides were detected with excitation at 320 nm and emission at 400 nm.

(iv) Sugar composition analysis. PA-oligosaccharides were hydrolyzed in 4 M TFA at 100°C for 6 h in evacuated sealed tubes. After removal of TFA, the sugars liberated were concentrated to dryness in conical glass tubes. The released monosaccharides in the residue were determined according to Takemoto *et al.* (22). Sialic acid was determined by the resorcinol method with *N*-acetylneuraminic acid as a standard (23). Sialic acid analysis was carried out according to Hara *et al.* (24).

(v) Glycosidase digestions. PA-oligosaccharides were digested with sialidase (*A. ureafaciens*), α2,3-sialidase (*S. typhimurium*), α-L-fucosidase (bovine kidney), β-galactosidase (jack bean and bovine testes), lacto-*N*-biosidase (*Streptomyces* sp.), β-*N*-acetyl-hexosaminidase (jack bean), or α-mannosidase (jack bean). The digestions with sialidase (10 mU) and α-L-fucosidase (10 mU) were performed in 25 μl of 50 mM sodium acetate buffer (pH 5.0) at 37°C for 24 h. Treatment with α2,3-sialidase (10 mU), two kinds of β-galactosidase (10 mU), lacto-*N*-biosidase (5 μU), β-*N*-acetyl-hexosaminidase (10 mU), and α-mannosidase (10 mU) was performed in 25 μl of 50 mM sodium acetate buffer (pH 5.5) at 37°C for 24 h.

(vi) Two-step digestion of monosialo PA-oligosaccharides. Monosialo PA-oligosaccharides were digested with β-galactosidase (10 mU, bovine testes) and β-*N*-acetyl-hexosaminidase (10 mU) in 25 μl of 50 mM sodium acetate buffer (pH 5.5) at 37°C for 24 h. After stopping the reaction by boiling for 3 min, sialidase (10 mU) and β-galactosidase (10 mU, bovine testes) were added to the reaction mixture and then incubated at 37°C for 24 h. Each digest was analyzed by the 2-D HPLC mapping method.

RESULTS AND DISCUSSION

Sequence Analysis of Rhodostoxin

Rhodostoxin was reduced and pyridylethylated prior to sequence analysis. The HPLC peptide map of rhodostoxin digested by endoproteinase Lys C is shown in Fig. 1. Sequence analysis of these peptides confirmed the deduced amino acid sequence of the putative hemorrhagic protein encoded by the prorhodostomin cDNA from *C. rhodostoma* (25, 26) (Fig. 2). However, the N-terminal residue should be asparagine (residue 113 of the translated sequence) instead of valine (residue 125 of the translated sequence) based on N-terminal sequencing of the purified protein (27). The amino acid sequencing results also revealed that residue 99 is a threonine instead of methionine (Fig. 2). The corresponding residue in most other snake venom metalloproteinases is also a threonine, thus suggesting that the difference could be due to a minor error in the cDNA sequence determination or possibly a point mutation. Therefore, rhodostoxin is a 203-amino acid residue protein with a calculated M_r of 23,438. It belongs to class I (small toxins with molecular weights of 20–30,000) of snake venom hemorrhagins (2). However, it exhibited potent hemorrhagic activity (27), in contrast to the widely held notion that the low-molecular-weight (class I) hemorrhagins are very weakly hemorrhagic (2).

A comparison of the amino acid sequence of rhodostoxin with the corresponding sequences of some of the published snake venom metalloproteinases revealed that rhodostoxin has the highest identity (54%) with the metalloproteinase domain of Ht-e from *Crotalus atrox* venom (10), followed by a 50% homology with the metalloproteinase domains of the high-molecular-weight HR1B from *Trimeresurus flavoviridis* venom (7) and jarrahagin from *Bothrops jararaca* venom (12) (results not shown). However, it is interesting to note that the phylogenetic tree of snake venom metalloproteinases indicates that rhodostoxin is least related to the other metalloproteinases, exhibiting only 33.7% identity (Fig. 3).

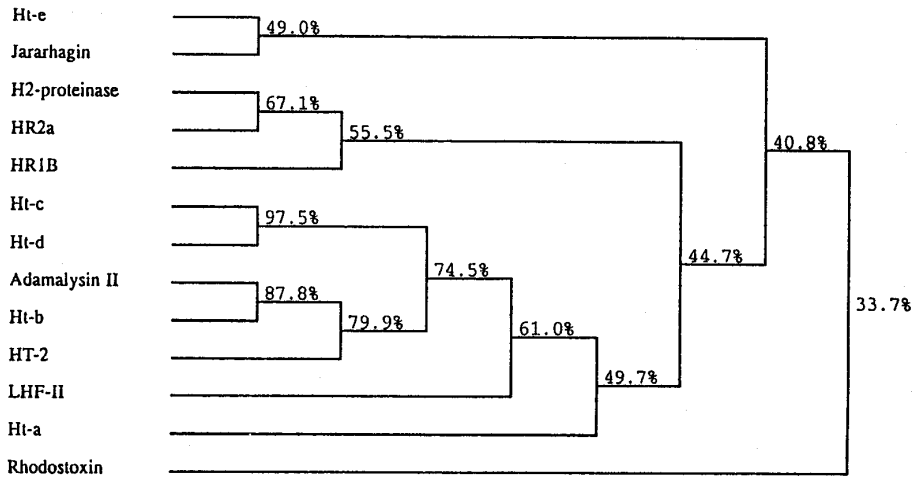

FIG. 3. Phylogenetic relationship of snake venom metalloproteinases. The phylogenetic tree was obtained based on the amino acid sequences of the metalloproteinases, using the Higgins–Sharp multiple alignment program in MacDNASIS. Calculated matching percentages between (among) the sequences are indicated at each branch point of the dendogram. References for the hemorrhagic snake venom metalloproteinases include rhodostoxin (this work); HR2a (4) and HR1B (7) from *Trimeresurus flavoviridis* venom; HT-2 (8) from *Crotalus ruber ruber* venom; LHF-II (9) from *Lachesis muta muta* venom; Ht-a, Ht-b, Ht-c (11), Ht-d (5), and Ht-e (10) from *Crotalus atrox* venom; and Jararhagin (12) from *Bothrops jararaca* venom. References for the nonhemorrhagic snake venom metalloproteinases include H2-proteinase (6) from *T. flavoviridis* venom and adamalysin II (29) from *Crotalus adamanteus* venom. Only the metalloproteinase domains of Ht-a, HR1B, and jararhagin were considered in this prediction.

Disulfide Bridges in Rhodostoxin

There are eight cysteine residues, none of which is present as free cysteine in the primary sequence of rhodostoxin. Chemical cleavage by cyanogen bromide produced two peptides, CN1 and CN2 (Fig. 4a), which upon enzymatic proteolysis by trypsin gave rise to cystine-linked peptide peaks CN1-T1 and CN1-T2, and CN2-T1, respectively (Figs. 4b and 4c). Sequencing of these peptides was used to identify the disulfide linkages. Peak CN1-T1 contained two peptides: A-Y-L-D-S-I-**X**-D-P-E-R (residues 111–121) and Y-I-E-N-Q-N-P-Q-**X**-I-L-N-K (residues 190–202). X in residues 117 and 198 corresponds to PE-Cys in the reduced and pyridylethylated protein (Fig. 2), thus suggesting a disulfide linkage between Cys117 and Cys198.

Peak CN1-T2 also contained two peptides: H-D-G-E-Y-**X**-T-**X**-Y-G-S-S-E-**X**-I-M (residues 152–167) and Y-F-S-N-**X**-S-Y-Y-Q-F-W-K (residues 178–189). Similarly, X in residues 157, 159, 165, and 182 corresponds to PE-Cys (Fig. 2). Attempts to further cleave the peptide-containing residues (152–167) with other enzymes (α-chymotyrpsin, thermolysin) to determine which of the three cysteine residues form a S–S linkage with peptide-containing residues (178–189) were unsuccessful. However, based on sequence homology with the disulfide bridges of the hemorrhagin HR2a from *T. flavoviridis* (4), the disulfide linkages can be deduced to be between Cys157 and Cys182 and between Cys159 and Cys165.

Peak CN2-T1 contained the following peptides: F-**X**-T-K (residues 18–21) and H-F-G-I-S-L-V-N-L-E-T-W-**X**-N-G-D-L-I-N-V-Q-E-D-S-Y-E-T-L-K (residues 48–76), thus indicating a disulfide linkage between Cys19 and Cys60. The results are summarized in Fig. 2. It is interesting to note that rhodostoxin contained four disulfide linkages, the novel disulfide linkage being Cys19–Cys60. This is in contrast to other known snake venom metalloproteinases where they are either "two-disulfide proteinases" or "three-disulfide proteinases" (28). In the two-disulfide proteinases the linkage is between Cys117 and Cys197 and Cys157 and Cys164, while the three-disulfide proteinases have disulfide connectivities between Cys157 and Cys181 and Cys 159 and Cys 164 in their "lower domain" in addition to the Cys 117–Cys 197 linkage. The X-ray crystal structure of adamalysin II, a two-disulfide proteinase, has recently been reported (28, 29), and it was stated that the disulfide connectivity in the three-disulfide proteinase would require some conformatinal shifts in the lower domain of the protein. With the additional fourth disulfide linkage in Cys19–Cys60, it is speculated that similar conformational shifts in the upper domain of rhodostoxin may result when compared to the structure of adamalysin II.

Glycosylation Sites of Rhodostoxin

Rhodostoxin is a glycoprotein with a carbohydrate content of 15%. The molecular weight of deglycosylated rhodostoxin, as determined by SDS–PAGE, was 24,000, in close agreement with the calculated molecular weight of 23,438, based on the amino acid sequence of the protein.

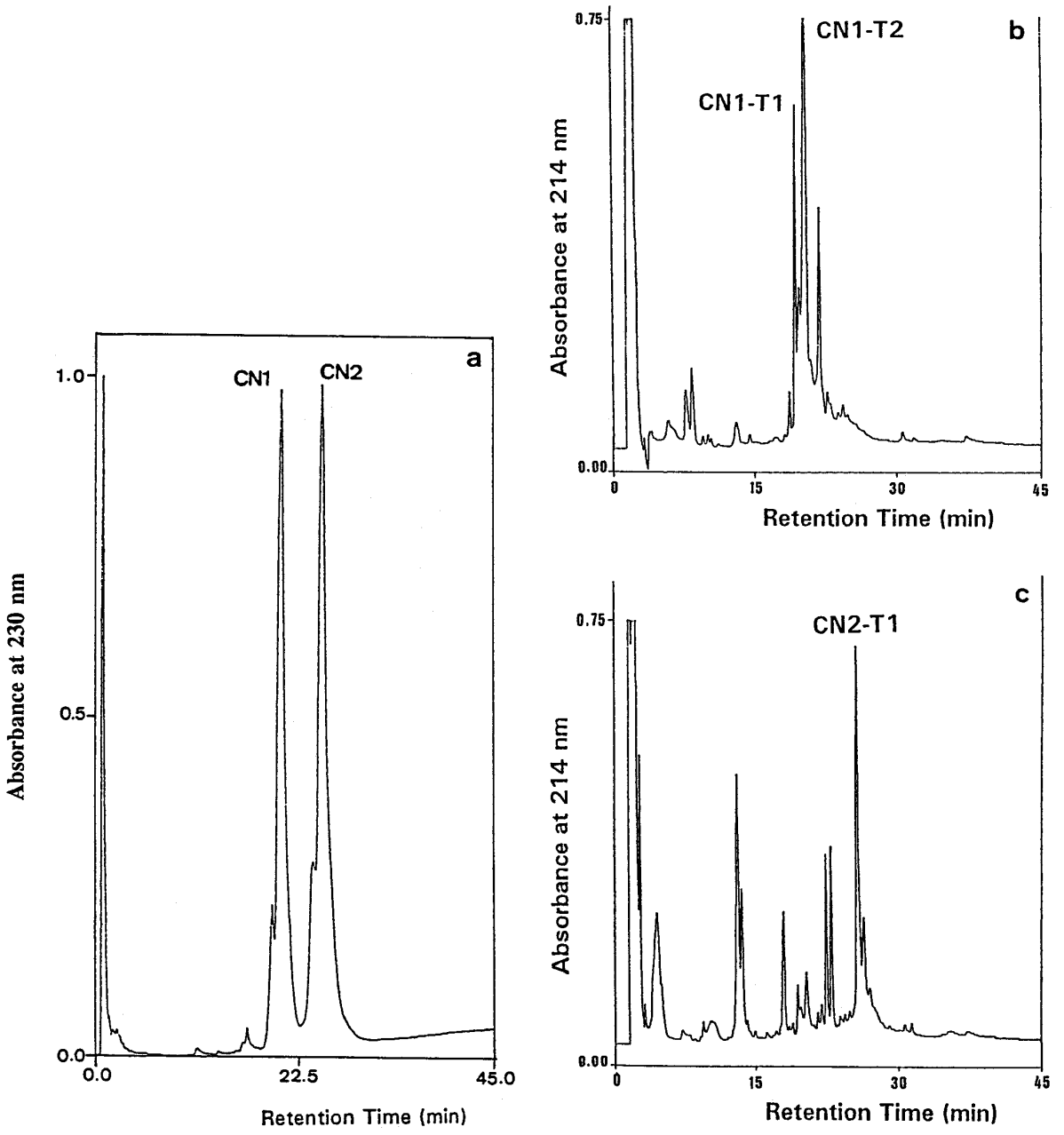

FIG. 4. HPLC elution profiles of (a) cyanogen bromide digest of rhodostoxin and (b) and (c) tryptic peptides of CN-1 and CN-2, respectively. See relevant section under Materials and Methods for details.

Dot-blotting results (not shown here) showed that peptides K-9 and K-14 (Fig. 1) gave positive staining with the carbohydrate detection kit. The DNA translated sequence revealed that both these peptides contained potential N-glycosylation sites with the consensus amino sequence of N-X-S/T (where X is any amino acid) (30). During automated amino acid sequencing, the third cycle in peptide K-9 (residue 91) (H-V-**X**-H-S-N-A-Q-F-L-T-D-M-K) and the fourth cycle in peptide K-14 (residue 181) (Y-F-S-**X**-C-S-Y-Y-Q-F-W-K) gave a "blank," suggesting the presence of posttranslationally modified residues. This is further confirmed by sequencing of the deglycosylated peptides K-9 and K-14, where the previous blank cycles now showed the presence of aspartic acid residues. Among the hemorrhagins studied thus far, only the high-molecular-weight HR1B from *T. flavoviridis* venom has been reported to be glycosylated with two Asn-linked sugar chains in the metalloproteinase domain attached to residues 73 and 181 (7). Another two N-linked sugar chains are

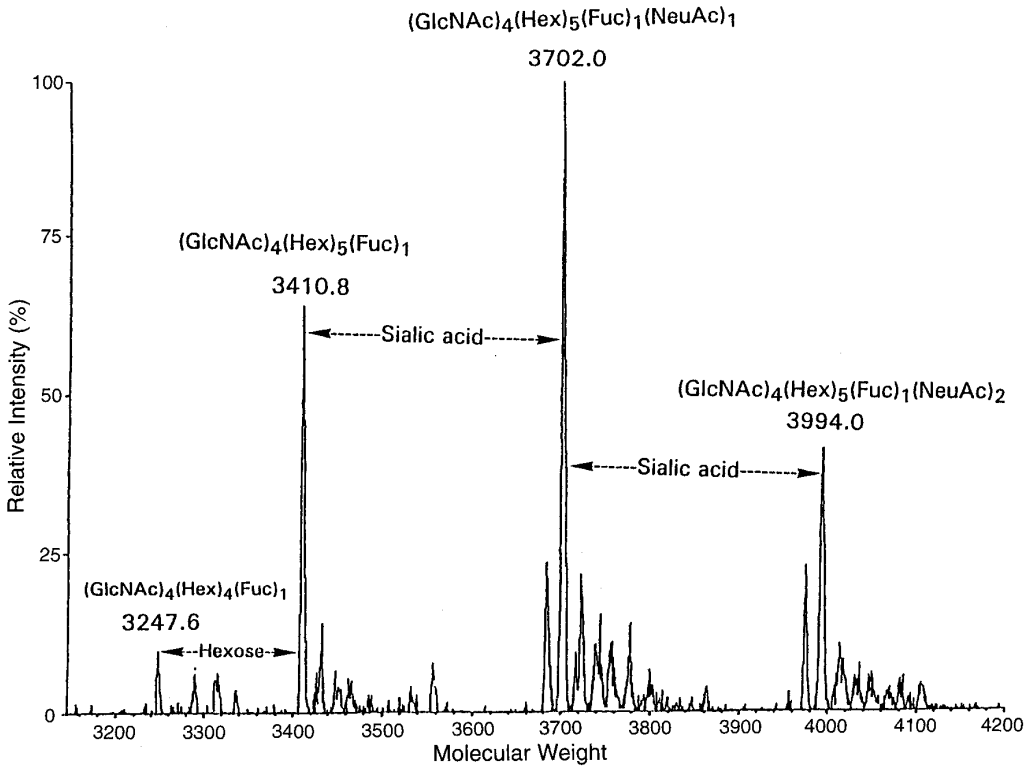

FIG. 5. Mass spectrometric analysis of glycopeptide K-9 isolated from endoproteinase digestion of pyridylethylated rhodostoxin.

found in the cysteine-rich carboxyl-terminal region. On the other hand, although HR2a and H2-proteinase from *T. flavoviridis* venom and LHF-II from *Lachesis muta muta* venom contained potential N-linked glycosylation sites in residues 103–105 (-N-F-T-), 72–74 (-N-V-T-), and 70–72 (-N-D-T-), respectively, no carbohydrate moiety had been detected in these proteins (4, 6, 9). Thus, rhodostoxin is the first low-molecular-weight hemorrhagic protein that has been shown to be fully glycosylated.

Mass Spectrometric Analysis

Peptides K-9 and K-14 (Fig. 1) were analyzed by mass spectrometry, and the spectrum for the former is presented in Fig. 5. The peak with a molecular weight of 3994.0 corresponds to a glycopeptide (peptide sequence H-V-N-H-S-N-A-Q-F-L-T-D-M-K, M_r 1642) containing an oligosaccharide structure containing 4 units of *N*-acetylglucosamine, 5 units of hexose, 1 unit of fucose, and 2 units of neuraminic acids. The peaks with molecular weights of 3702.0, 3410.8, and 3247.6 were consistent with the loss of one, two, and two neuraminic acids and one hexose from the above structure, respectively. However, it was not possible to determine the exact structure (linkage, anomeric configuration) of the oligosaccharide chain based on the above mass spectral results. An alternative approach was used to elucidate the glycan structure (see next section). The mass spectrometric data for glycopeptide K-14 gave similar results as glycopeptide K-9, thus suggesting that the two glycan moieties have similar structures.

Glycan Structure of Rhodostoxin

PA-oligosaccharides, when analyzed on a reverse-phase column, gave eight peaks (A–H) (Fig. 6a). However, when the mixture of PA-oligosaccharides was digested with sialidase and α-L-fucosidase separately, two peaks (A and E) and four peaks (A–D) were obtained, respectively (Figs. 6b and 6c). On the other hand, only peak A remained when the digestion was carried out with sialidase and α-L-fucosidase together (Fig. 6d). The amount of peak A in Fig. 6d was equivalent to the sum of all the oligosaccharides in Fig. 6a. These results suggested that peak A might contain the fundamental form of the oligosaccharide structure of rhodostoxin, while peaks B–D and F–H contained sialyl groups and peaks E–H contained fucosyl groups. The sugar composition (Table I) of each of the HPLC-purified PA-oligosaccharides confirmed this conclusion. The sialic acid present in rhodostoxin was shown to be *N*-acetylneuraminic acid based on the retention time of the 1,2-diamino-4,5-methylenedioxybenzene–sialic acid (24).

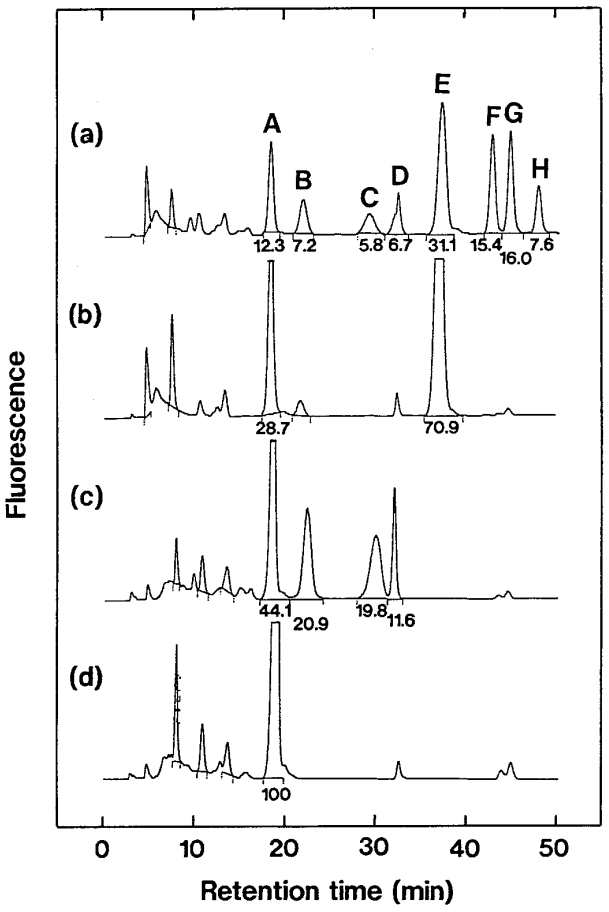

FIG. 6. Reverse-phase HPLC analysis of PA-oligosaccharides from rhodostoxin and their exoglycosidase digests. The conditions are given under Materials and Methods. (a) Intact, (b) sialidase digest, (c) α-L-fucosidase digest, and (d) sialidase and α-L-fucosidase digests. Numbers under the peaks express the relative fluorescence intensity of each peak as a percentage of peak A in d.

To study the structure of each PA-oligosaccharide, the individual peak was digested with various exoglycosidases and the resulting digest analyzed by 2-D mapping (21). These results are summarized in Table II. It was found that the elution positions of the eight PA-oligosaccharides isolated from rhodostoxin did not coincide with any of the hitherto reported PA-oligosaccharides. However, from the results of sialidase digestion, PA-oligosaccharides A and E are asialo forms of PA-oligosaccharides B–D and PA-oligosaccharides F–H, respectively. The results of α-L-fucosidase digestion suggest that PA-oligosaccharides A–D are defucosyl forms of PA-oligosaccharides E–H, respectively. Furthermore, since (α2-3)-specific sialidase (*S. typhimurium*) digestion showed the same results as nonspecific sialidase (*A. ureafaciens*) digestion, all sialyl bonds of oligosaccharides B–D and F–H are of the α2,3 type.

On incubation of each PA-oligosaccharide with exoglycosidases other than sialidase and α-L-fucosidase, only oligosaccharides A and E were digested by β-galactosidase (bovine testes) or lacto-*N*-biosidase. The elution positions of each of these digested PA-oligosaccharides coincided with that of the already-known PA-oligosaccharides (200.1, 210.1, 000.1, and 010.1) on 2-D mapping (Table II, see Fig. 7). To confirm this observation, further digestion of these four PA-oligosaccharides with β-*N*-acetyl-hexosaminidase, α-mannosidase, and/or α-L-fucosidase was carried out. All of them were digested to Manβ1-4GlcNAcβ1-4GlcNAc-PA (M1.1) through expected routes (Fig. 7). As shown in Table II, due to the resistance of PA-oligosaccharides A and E to (β1-4)-specific galactosidase (jack bean) and their sensitivity to β-galactosidase (bovine testes) and lacto-*N*-biosidase (liberating Galβ1-3GlcNAc), galactose might be linked to C-3 of GlcNAc, thus forming a type-1 lactosamine antenna. These results, together with the sugar composition (Table I), led us to propose that the sugar sequences of PA-oligosaccharides A, D, E, and H might be those of structure Nos. 1, 4, 5, and 8 shown in Fig. 8, while PA-oligosaccharides B and C and F and G might be structure Nos. 2 or 3 and 6 or 7, respectively. To resolve these ambiguities, the monosialo PA-oligosaccharides (B, C, F, and G) were subjected to a further two-step exoglycosidase digestion procedure. After digestion, PA-oligosaccharides B, C, F, and G were converted to the known PA-oligosaccharides, 100.2, 100.1, 110.2, and 110.1, respectively, on 2-D mapping (21). These results suggested that the sugar sequences of PA-oligosaccharides B, C, F, and G might be those of structure Nos. 3, 2, 7, and 6 shown in Fig. 8, respectively.

Structure 8 (Fig. 8) represents the complete oligosaccharide structure of the glycan chain of rhodostoxin. It is a N-linked complex type of carbohydrate structure with novel 2,3-linked sialic acids and Galβ(1-3)GlcNAc linkages. The structure is consistent with the carbohydrate compositions of glycopep-

TABLE I

Sugar Compositions of PA-Oligosaccharides

	Man	Fuc	Gal	GlcNAc	Sia
A	3.0	ND	2.1	3.8	ND
B	3.0	ND	1.9	3.9	0.9
C	3.0	ND	2.0	3.8	1.1
D	3.0	ND	2.0	4.0	2.2
E	3.0	1.1	2.2	3.9	ND
F	3.0	1.0	2.1	3.8	1.0
G	3.0	1.1	1.9	3.9	1.2
H	3.0	1.0	2.0	3.8	2.1

Note. Values are expressed as molar ratios to mannose as 3.0. ND, not detected.

TABLE II

Exoglycosidase Digestion of PA-Oligosaccharides from Hemorrhagin

PA-oligosaccharides	A	B	C	D	E	F	G	H
Control	8.5 × 6.7	9.4 × 6.2	10.3 × 6.2	10.9 × 5.8	11.6 × 7.1	13.0 × 6.7	13.6 × 6.7	14.6 × 6.2
Sialidase (*A. ureafaciens*)	—	8.5 × 6.7	8.5 × 6.7	8.5 × 6.7	—	11.6 × 7.1	11.6 × 7.1	11.6 × 7.1
α2,3-Sialidase (*S. typhimurium*)	—	8.5 × 6.7	8.5 × 6.7	8.5 × 6.7	—	11.6 × 7.1	11.6 × 7.1	11.6 × 7.1
α-L-Fucosidase (bovine kidney)	—	—	—	—	8.5 × 6.7	9.4 × 6.2	10.3 × 6.2	10.9 × 5.8
β-Galactosidase (jack bean)	—	—	—	—	—	—	—	—
β-Galactosidase (bovine testes)	8.9 × 5.1 (200.1)	—	—	—	12.3 × 5.5 (210.1)	—	—	—
Lacto-*N*-biosidase (*Streptomyces* sp.)	7.4 × 4.3 (000.1)	—	—	—	10.2 × 4.7 (010.1)	—	—	—
β-*N*-acetyl-hexosaminidase (jack bean)	—	—	—	—	—	—	—	—
α-Mannosidase (jack bean)	—	—	—	—	—	—	—	—

Note. Each PA-oligosaccharide was digested with various exoglycosidases as described under Materials and Methods. Each digest was analyzed with the 2-D mapping method. Elution positions on HPLC columns are expressed as the number of glucose units of the corresponding standard glucose oligomers as ODS × amide. Numbers in parentheses show already-known PA-oligosaccharides [see Ref. (21)]. —, no change.

tides K-9 and K-16 as determined by mass spectrometry. It is the first report of a complete oligosaccharide structure for hemorrhagic proteins. Although many venom proteins are glycosylated, the structures of their carbohydrate moieties are largely unknown. Recently, some qualitative studies on the structural features of carbohydrate moieties in snake venom glycoproteins have been reported (31). In earlier work, it has been reported that the high-molecular-weight hemorrhagin from *T. flavoviridis*, HR1B, contained neutral sugars, amino sugars, and silaic acids (32), and the hemorrhagic toxins from *Crotalus viridis viridis* possessed Galβ(1-4)GlcNAc side chains as determined by a glycan differentiation kit (33). It is interesting to note that the oligosaccharide structure of rhodostoxin is very similar to the carbohydrate chain of the thrombin-like serine protease ancrod isolated from the venom of the same snake (former name *Agkristrodon rhodostoma*) (34). However, it differs from that of the carbohydrate chain of another thrombin-like enzyme, batroxobin, isolated from *Bothrops atrox moojeni* venom (35). This observation is consistent with the report that snake venom proteins are glycosylated in a species-specific manner and appear to contain oligosaccharides with novel and diverse structures (31).

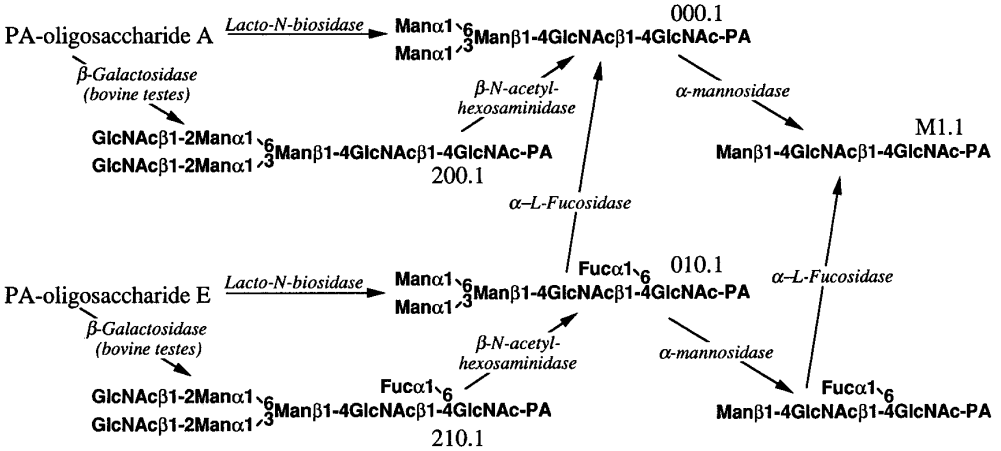

FIG. 7. Exoglycosidase digestion of PA-oligosaccharides A and E. The conditions are given under Materials and Methods. Each digest was analyzed by the 2-D mapping method.

No.	Structures
1	Galβ1-3GlcNAcβ1-2Manα1↘6 Galβ1-3GlcNAcβ1-2Manα1↗3Manβ1-4GlcNAcβ1-4GlcNAc-PA
2	NeuAcα2-3Galβ1-3GlcNAcβ1-2Manα1↘6 Galβ1-3GlcNAcβ1-2Manα1↗3Manβ1-4GlcNAcβ1-4GlcNAc-PA
3	Galβ1-3GlcNAcβ1-2Manα1↘6 NeuAcα2-3Galβ1-3GlcNAcβ1-2Manα1↗3Manβ1-4GlcNAcβ1-4GlcNAc-PA
4	NeuAcα2-3Galβ1-3GlcNAcβ1-2Manα1↘6 NeuAcα2-3Galβ1-3GlcNAcβ1-2Manα1↗3Manβ1-4GlcNAcβ1-4GlcNAc-PA
5	Fucα1↘6 Galβ1-3GlcNAcβ1-2Manα1↘6 Galβ1-3GlcNAcβ1-2Manα1↗3Manβ1-4GlcNAcβ1-4GlcNAc-PA
6	Fucα1↘6 NeuAcα2-3Galβ1-3GlcNAcβ1-2Manα1↘6 Galβ1-3GlcNAcβ1-2Manα1↗3Manβ1-4GlcNAcβ1-4GlcNAc-PA
7	Fucα1↘6 Galβ1-3GlcNAcβ1-2Manα1↘6 NeuAcα2-3Galβ1-3GlcNAcβ1-2Manα1↗3Manβ1-4GlcNAcβ1-4GlcNAc-PA
8	Fucα1↘6 NeuAcα2-3Galβ1-3GlcNAcβ1-2Manα1↘6 NeuAcα2-3Galβ1-3GlcNAcβ1-2Manα1↗3Manβ1-4GlcNAcβ1-4GlcNAc-PA

FIG. 8. The structures of PA-oligosaccharides from rhodostoxin.

ACKNOWLEDGMENTS

We acknowledge Jun Chen for her skillful assistance in the peptide-mapping experiments and Mr. S. Nimkar of Perkin–Elmer (Singapore) for mass spectrometric analyses. This work was supported by Research Grant IRPA 3-07-04-097 from the Government of Malaysia.

REFERENCES

1. Kini, R. M., and Evans, H. J. (1992) *Toxicon* **30,** 265–293.
2. Bjarnason, J. B., and Fox, J. W. (1989) *J. Toxicol. Toxin Rev.* **7,** 121–209.
3. Ohsaka, A. (1979) *in* Handbook of Experimental Pharmacology (Lee, C. Y., Ed.), Vol. 5, pp. 480–546, Springer-Verlag, Berlin.
4. Miyata, T., Yakeya, H., Ozeki, Y., Arakawa, M., Tokunaga, F., Iwanaga, S., and Omori-Satoh, T. (1989) *J. Biochem.* **105,** 847–853.
5. Shannon, J. D., Baramove, E. N., Bjarnason, J. B., and Fox, J. W. (1989) *J. Biol. Chem.* **264,** 175–190.
6. Takeya, H., Arakawa, M., Miyata, T., Iwanaga, S., and Omori-Satoh, T. (1989) *J. Biochem.* **106,** 151–157.
7. Takeya, H., Oda, K., Miyata, T., Omori-Satoh, T., and Iwanaga, S. (1990) *J. Biol. Chem.* **265,** 16068–16073.
8. Takeya, H., Onikura, A., Nikai, T., Sugihara, H., and Iwanaga, S. (1990) *J. Biochem.* **108,** 711–719.
9. Sanchez, E. F., Diniz, C. R., and Richardson, M. (1991) *FEBS Lett.* **282,** 178–182.
10. Hite, L. A., Shannon, J. D., Bjarnason, J. B., and Fox, J. W. (1992) *Biochemistry* **31,** 6203–6211.
11. Hite, L. A., Jia, L. G., Bjarnason, J. B., and Fox, J. W. (1994) *Arch. Biochem. Biophys.* **308,** 182–191.
12. Paine, M. J. I., Desmond, H. P., Theakston, R. D. G., and Crampton, J. M. (1992) *J. Biol. Chem.* **267,** 22869–22876.
13. Dupont, D., Keim, P., Chui, A., Bello, R., and Wilson, K. (1987) Applied Biosystems User Bulletin, No. 1, pp. 1–7.
14. Aitken, A., Geisow, M. J., Findlay, J. B. C., Holmes, C., and Yarwood, A. (1989) *in* Protein Sequencing: A Practical Approach (Findlay, J. B. C., and Geisow, A., Eds.), pp. 43–68, IRL Press, UK.
15. Kirley, T. L. (1989) *Anal. Biochem.* **180,** 231–236.
16. Spiro, R. G. (1966) *in* Methods in Enzymology (Neufeld, E. F., and Ginsburg, U., Eds.), Vol. 8, pp. 3–5, Academic Press, London.
17. Laemmli, U. K. (1970) *Nature* **227,** 680–685.
18. Canas, B., Dai, Z., Lackland, H., Poretz, R., and Stein, S. (1993) *Anal. Biochem.* **211,** 179–182.
19. Hsi, K. L., Chen, L., Hawke, D. H., Zieske, L. R., and Yuan, P. M. (1991) *Anal. Biochem.* **198,** 238–245.
20. Hase, S., Ibuki, S., and Ikenaka, T. (1984) *J. Biochem.* **95,** 197–203.
21. Tomiya, N., Awaya, J., Kurono, M., Endo, S., Arata, Y., and Takahashi, N. (1988) *Anal. Biochem.* **171,** 73–90.
22. Takemoto, H., Hase, S., and Ikenaka, T. (1985) *Anal. Biochem.* **145,** 245–250.
23. Jourdian, G. W., Dean, L., and Roseman, S. (1971) *J. Biol. Chem.* **246,** 430–435.

24. Hara, S., Yamaguchi, M., Takemori, Y., Furuhata, K., Ogura, H., and Nakamura, M. (1989) *Anal. Biochem.* **179,** 162–166.
25. Au, L. C., Huang, Y. B., Huang, T. F., Teh, G. W., Lin, H. H., and Choo, K. B. (1991) *Biochem. Biophys. Res. Commun.* **181,** 585–593.
26. Au, L. C., Chou, J. S., Chang, K. J., Teh, G. W., and Lin, S. B. (1993) *Biochim. Biophys. Acta* **1173,** 243–245.
27. Ponnudurai, G., Chung, M. C. M., and Tan, N. H. (1993) *Toxicon* **31,** 997–1005.
28. Gomis-Ruth, F. X., Kress, L. F., and Bode, W. (1993) *EMBO J.* **12,** 4151–4157.
29. Gomis-Ruth, F. X., Kress, L. F., Kellermann, J., Mayr, I., Lee, X., Huber, R., and Bode, W. (1994) *J. Mol. Biol.* **239,** 513–544.
30. Kornfeld, R., and Kornfeld, S. (1985) *Annu. Rev. Biochem.* **54,** 631–664.
31. Gowda, D., and Davidson, E. A. (1992) *Biochem. Biophys. Res. Commun.* **182,** 294–301.
32. Omori-Satoh, T., and Sadahiro, S. (1979) *Biochim. Biophys. Acta* **580,** 392–404.
33. Li, Q., Colberg, T. R., and Ownby, C. L. (1993) *Toxicon* **31,** 711–722.
34. Pfeifer, G., Dabrowski, U., Dabrowski, J., Stirm, S., Strube, K. H., and Geyer, R. (1992) *Eur. J. Biochem.* **205,** 961–978.
35. Tanaka, N., Nakada, H., Itoh, N., Mizuno, Y., Takanishi, M., Kawasaki, T., Tate, S., Inagaki, F., and Yamashina, I. (1992) *J. Biochem.* **112,** 68–74.